INTERNATIONAL JOURNAL of RENEWABLE ENERGY RESEARCH
Sugiyanto et al., Vol.9, No.3, September, 2019

The Experimental Study of Bi-Directional Impulse Turbine on Standing Wave Thermoacoustic Engine

Sugiyanto*‡, Samsul Kamal**, Joko Waluyo***, Adhika Widyaparaga****

* Ph.D. Candidate in Department of Mechanical and Industrial Engineering, Faculty of Engineering, Gadjah Mada University, Jl. Teknika Utara, Yogyakarta, Indonesia, 55281

* Department of Mechanical Engineering, Vocational School, Gadjah Mada University, Jl. Grafika 2a, Yogyakarta, Indonesia, 55281

** Department of Mechanical and Industrial Engineering, Faculty of Engineering, Gadjah Mada University, Jl. Teknika Utara, Yogyakarta, Indonesia, 55281

*** Department of Mechanical and Industrial Engineering, Faculty of Engineering, Gadjah Mada University, Jl. Teknika Utara, Yogyakarta, Indonesia, 55281

*** Department of Mechanical and Industrial Engineering, Faculty of Engineering, Gadjah Mada University, Jl. Teknika Utara, Yogyakarta, Indonesia, 55281

(sugiyanto_t@ugm.ac.id, samsul@ugm.ac.id, jokowaluyo@ugm.ac.id, adhika@ugm.ac.id)

‡ Corresponding Author; Sugiyanto, Department of Mechanical and Industrial Engineering, Faculty of Engineering, Gadjah Mada University, Jl. Teknika Utara, Yogyakarta, Indonesia, 55281, Tel: +62 8112502021,

sugiyanto_t@ugm.ac.id

Received: 27.05.2019 Accepted:03.08.2019

Abstract- Bi-directional air turbine has one of the primary functions, namely changing the linear movement of air into a rotating motion. This rotating motion is always in the same direction regardless of the direction of air movement. This bi-directional turbine impulse type moves by using thermoacoustic waves which result from the conversion of heat energy into acoustic energy. The turbine using in this research has a diameter of 48 mm and 50 mm. Besides, the turbine also has a variety of blade numbers and variations of distance from the sound source. The impulse turbine research with 50º inlet angle obtained results that the maximum rotational motion in the turbine with a diameter of 50 mm and the number of blades 28. The optimal results were purchased at a distance of 200 mm from the sound source, which was 361 rpm.

Keywords Bi-directional Impulse Turbine; Thermoacoustic Engine; Heat Conversion; Acoustic Power; Rotational Motion.

1. Introduction

Technology that can utilize waste heat directly as an energy source to be converted into mechanical energy and electrical energy, one of which is thermoacoustic technology. Thermoacoustic is a branch of science that studies the conversion of heat energy into sound energy and vice versa [1]. The sound energy produced can be used as a power plant, refrigerator, or heat pump. The utilization of industrial heat waste as a heat source in a thermoacoustic heat engine was examined by [2]. Thermo Acoustic Power (TAP)-4 stages are designed to convert 100 kW of flue gas heat energy at 150 ºC - 160 ºC to 10 kW of electrical energy. The use of heat recoveries with thermoacoustic heat engines (TAHEs) in the food industry is carried out by [3], the results of the simulation are that the machine can utilize waste heat in the food industry to 1029.10W acoustic power with an efficiency of 5.42%. The waste heat from the exhaust gases of gasoline-powered vehicles is realized by [4] which directly utilizes heat on the muffler as a hot heat exchanger source on the thermoacoustic engine as well as the use of electric heaters for laboratory-scale thermoacoustic. The utilization of waste gas heat waste in small trucks is performed by [5], with the optimum temperature of vehicles 300 ^{o}C – 350 ^{o}C capable of producing 220 W of electrical energy for small engines and 490 W for larger machines.

The use of thermoacoustic acoustic energy to be converted into electrical power has been implemented by several researchers, mainly by using both linear and rotary alternators. A pair of linear alternators are paired by [6] on the walking wave resonator of the TASHE system. Another study using linear alternators was conducted by [7]. In 2012, [8] replaced linear alternators with commercial speakers. In the use of rotary alternators, acoustic wave energy is captured by a turbine blade system to be converted by the alternator. A multi-directional wave concept has been carried out in the form of an oscillating water column wave energy recovery system.

The concept of waves that can produce rotary motion of all directions has been applied to wave energy utilization systems with Oscillating Water Column (OWC). The reasons for using this device is the low operational cost, and the only moving part of the energy conversion mechanism are the rotors of a turbine [9]. The OWC has an open chamber which is in direct contact with the sea so that incoming and outgoing waves cause the water level in the chamber to rise and fall. Changes in water level produce a bi-directional airflow that can drive the Wells turbine connected directly to an electrical generator [10] or use a direct-link mechanism that to be used in an interconnected wave generation system with a power converter and a battery [11]. The counter-rotating impulse turbine is used by [12] to convert wave energy in an OWC with computation fluid dynamics (CFD) analysis.

A Wells turbine has a simple geometric shape, so it can be said that this type of turbine is one of the most accessible forms of bi-directional turbines and is very economical. However, a Wells turbine has the disadvantage of being a bad self-starting, and its efficiency in an OWC is only 30% [13]. Compared to the capability of the impulse turbine which has an efficiency of 40-50% [13] and can even reach 70% at optimal conditions [14], the turbine impulse has more efficiency advantages than a Wells turbine. The turbine is a device that needs to be improved to support decentralization of energy, especially in remote places far from the power station [15]. How to increase the turbine power output has been done by [16], namely the non-linear speed regulation scheme of OWC with Wells turbine and doubly-fed induction generator (DFIG). Another way to increase the turbine power output is to use the Wells turbine and the impulse turbine simultaneously in an OWC. Wells turbine as the main turbine that will capture oscillating airflow while Impulse turbine as a booster [17].

The moving air in an OWC due to waves is comparable to the sound waves in a thermo-acoustic system. From the results of existing research in terms of converting a linear into a rotating motion using a bi-directional turbine, axial turbines are widely used, namely wells turbine and impulse axial turbines [18]. The use of thermoacoustic as a bi-directional turbine driving source was carried out by [19] and [20]. Both of them use audio loudspeakers as energy sources that produce turbine drive waves, while this research uses a thermoacoustic engine as its energy source. The advantage of the thermoacoustic engine is that it has relatively few components; there are no moving parts and does not require refrigerants or hazardous chemicals. Air can be used as a working fluid, which is very friendly to the environment [21]. Then, the cost of fabrication and maintenance is relatively low because the equipment is straightforward. In this study, the type of turbine used is an impulse turbine with 50º inlet angle, and the hub-to-tip ratio is equal to 0.6. The nominal diameter of the turbine used is 48 mm and 50 mm, each of which has a variation of the number of blades (Z) of 26, 28 and 30. This study characterizes the effectiveness of bi-directional impulse turbine for use with a thermoacoustic engine; which is a technology that uses an induced temperature gradient to propagate acoustic waves within a resonator [22].

2. Theoretical Basis

Impulses Turbine is paired inside the resonator of thermoacoustic engine to convert a linear movement of the sound wave into a rotating motion of the turbine. The impulse turbine has a profile like a water mill, where a blade in the form of an aerodynamic curve aims to convert the airflow into a rotational motion of the turbine, as seen in Fig 1. Essential design aspects include the diameter of the turbine, the number of blades, and hub-to-tip ratio.

The number of blades is based on the review of previous studies, which are 30 [23], [13]. The hub-to-tip ratio is the ratio between the diameter of the inside and the outside of the turbine blades. The hub-to-tip ratio is essential for determining turbine performance. When the hub diameter is more significant, the blade section becomes smaller so that it can increase air motion. A hub-to-tip ratio of 0.6 give superior performance [24]. Blade size is determined by the blade inlet angle and shape curvature. The 60º blade inlet angle is most commonly used in wave energy applications that were previously adjusted to the impulse turbine and thermoacoustic generator using the blade inlet angle of 67º. However for further research using blade angles of 50º, 60º, and 70º is designed for analysis [24].

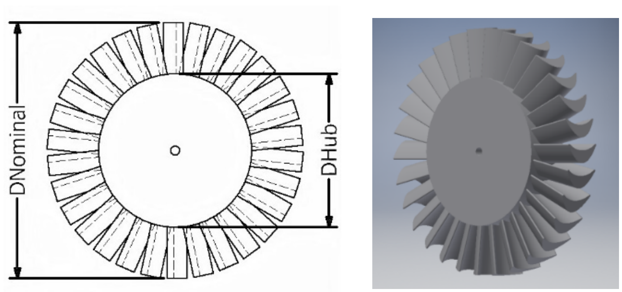

Fig. 1. An Impulse Turbine

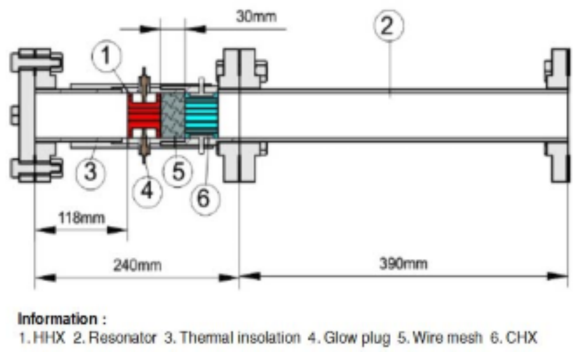

Fig. 2. Thermoacoustic Engine Schematic [25]

The thermoacoustic engine has the main components, namely hot heat exchanger (HHX), stack, a cold heat exchanger (CHX), and resonator as shown in Fig 2. The engine used is a close-open type with straight tubular and narrow inside diameter resonator. High temperature can be obtained from several sources such as industrial waste heat, motor vehicles, or commercial systems. In this laboratory-scale study as a heat source was taken from DC glowplug.

The stack is one of the essential components in the thermoacoustic engine. Thermal penetration depth is one of a characteristic length of this system that is perpendicular to the direction of motion of the gas. It defined as [22]:

$$\delta_k = \sqrt{\frac{2k}{\rho_m\, c_p\, \omega}} \tag{1}$$

with k is the thermal conductivity, ρ_m is the mean density, c_p is the constant specific pressure heat of the working gas, and ω is an angular frequency of the sound wave.

The other characteristic length is viscous penetration depth [22] :

$$\delta_v = \sqrt{\frac{2\mu}{\omega\, \rho_m}} = \sqrt{\frac{2v}{\omega}} \tag{2}$$

With μ is dynamic viscosity. Losses due to viscous effects occur in this region. The resonance frequency of the open-ended thermoacoustic engine is given by [26]:

$$f_{res} = \frac{a}{2L} = \sqrt{\left[\frac{\gamma RT}{M}\right]} \Big/ 2L \tag{3}$$

where a is the motion of sound, L is the resonator length, γ is the ratio of specific heat, R is the molar gas constant, T is absolute temperature, and M is the molar mass of gas.

The result of heat conversion on the thermoacoustic engine is the acoustic intensity (I) which can then be used to find the amount of acoustic power. The measurement and calculation of acoustic intensity can be done using the two sensor method. The acoustic intensity I for the measured sound wave was determined using the modified two sensor method [27]:

$$I = \frac{1}{8\omega\rho_m}\{Im[H](|P_A|^2 - |P_B|^2) + 2\, re[H]|P_A||P_B|\sin\theta\} \tag{4}$$

H is defined by:

$$H = \frac{kF}{\cos\left(k\frac{\Delta x}{2}\right) sin\left(k\frac{\Delta x}{2}\right)} \tag{5}$$

Where Re [ ] and Im [ ] represent the real and imaginary components. P_A and P_B are the pressure waves measured at adjacent pressure sensor positions along resonator, and θ = arg [P_A/P_B] represents phase lead of pressure wave P_A relative to P_B, k is a complex wavenumber, and F is a complex factor calculated by:

$$F = 1 - \frac{2J_1\left(i^{3/2}\sqrt{2r_0/\delta}\right)}{\left(i^{3/2}\sqrt{2r_0/\delta}\right)J_0\left(i^{3/2}\sqrt{2r_0/\delta}\right)} \tag{6}$$

Table. 1. Uncertainty in the measurement of sound levels according to ISO 9641-1: 1993 [28]

Octave band center frequencies [Hz]	One-third band center frequencies [Hz]	Standard deviation, s Engineering (grade 2) [dB]
63 to 125	50 to 160	3
250	200 to 315	2
500 to 4000	400 to 5000	1.5
	6300	2.5

$$k = -ik_0\sqrt{\frac{J_0 2J_1\left(i^{3/2}\sqrt{2r_0/\delta}\right)}{J_2 2J_1\left(i^{3/2}\sqrt{2r_0/\delta}\right)}}\sqrt{\gamma + (\gamma - 1)\frac{J_2\left(i^{3/2}\sqrt{2r_0/\delta}\right)}{J_0\left(i^{3/2}\sqrt{2r_0/\delta}\right)}} \tag{7}$$

Where γ and σ are the specific heat ratio and Prandtl number, J_n is the nth order complex Bessel function, k_0 is the wavenumber in free space given by ω divided by the adiabatic motion of sound, and r_0 is the radius of the duct.

While acoustic power ($\dot{E}$) can be calculated by multiplying the acoustic intensity (I) with the cross-sectional area of the resonator (A), that is, in the following equation:

$$\dot{E} = \mathrm{I \times A} \tag{8}$$

The measurement method of sound power using sound intensity is very difficult to evaluate the resulting measurement uncertainty because of the fact that intensity-based sound power measurements take place under widely different condition [28]. Uncertainty in the determination of sound power levels according to ISO 9614-1 can be seen in Table 1.

3. Experiment Setup

A close-open standing wave thermoacoustic engine (SWTE) with 630 mm total length used in this study, as seen in Fig. 3 consists of a cylindrical core with a copper hot heat exchanger (HHX) and cold heat exchanger (CHX). The HHX heated by 12 pcs glow plug of the diesel engine 11 VDC, and CHX cooled by water. A wire stack made of stainless steel wire mesh with porosity 88.26% is placed between HHX and CHX. The resonator is made from an acrylic tube with 390 mm length and the inner diameter of 52 mm.

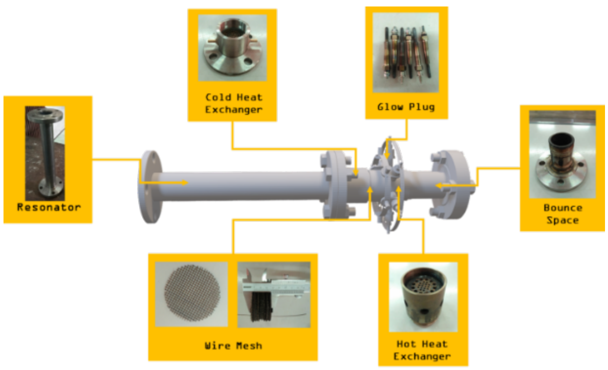

Fig. 3. Schematic diagram of a close-open thermoacoustic engine

Fig. 4 Three-dimensional printed models of Impulses turbine Dia. 48 and 50 mm with the variation of the number of blades.

Fig. 5. Test Apparatus

The parameters of the thermoacoustic engine selected for use in this study aim to obtain some performance quantities that can be used as bi-directional turbine drives. The use of glow plug can produce a temperature on the HHX side of 450 ^{o}C and a temperature on the CHX side of 30 ^{o}C or a temperature difference on the core side of 420 ^{o}C. The working frequency of the system based on the total engine length used will be more than 100 Hz, while the use of wire mesh with 88.26% porosity is chosen because the system works as a standing wave. The magnitude of the performance of the SWTE output has been able to generate acoustic intensity and acoustic power that is able to drive the turbine.

Hub-to-tip ratio is the ratio between the inside diameter and the outside of the turbine blades. Hub-to-tip ratio is essential to determine turbine performance. A hub-to-tip ratio of 0.6 was chosen to increase air velocity [19]. The turbine used in the test has a hub-to-tip ratio of 0.6 and diameter of with variations in the number of blades, namely 26, 28 and 30, while the variety of turbine's diameters are 48 and 50. Fig. 4 shows the three-dimensional printed models of turbines.

The test apparatus of impulses turbine inserted within the resonator of the thermoacoustic engine shown in Fig 5. The turbine tests are performed under different position inside the resonator, starting from the open end of the resonator, which is 350 mm from the end of the CHX. Subsequent testing varied the distance increase every 50 mm from the first test.

Data retrieval is done by the method of two sensors (PA and PB), which are used to calculate the intensity. The two-sensor method can be used to estimate the acoustic intensity between PA sensors and PB sensors by knowing the distance between the two. Two pressure transducers record the amplitude of the pressure and the phase difference of both. Then the calculation is done to obtain the acoustic intensity. Two sensors used to calculate acoustic power in this study used PA and PB pressure transducers. PA and PB pressure transducers have a distance of 50 mm; the distance between the two sensors is adjusted to the recommendations of [27].

4. Result And Discussion

The pressure transducer will produce raw data amplitude pressure versus time. The time-domain will be converted into the frequency domain by the FFT (Fast Fourier Transform) method that commonly used in waveform analysis [29] so that the pressure amplitude is obtained. Based on the test results can be obtained the value of pressure amplitude (PA) of 0.0043 kPa and a frequency of 125 Hz. While the amount of pressure amplitude (PB) is 3.6731 kPa, and the frequency is 125 Hz. Acoustic power is used to determine the performance of the tool. The acoustic intensity obtained was 20.9474 kW/m^2. From the 52 mm diameter and 390 mm length of resonator test data, acoustic power was obtained at 45.3114 Watts. The uncertainty of this measurement is 3 dB, according to Table 1.

The results of experimental tests when the turbine is driven by the thermoacoustic engine discussion as follows.

From Fig. 6, it can be seen that at a diameter of 50 mm the highest rotating motion is at a distance of 20 cm from the sound source, which is equal to 269 rpm. While for the lowest rotational motion is at a length of 350 mm from the sound source, which is 217 rpm. From the graph, it can be seen that the impulse turbine motion tends that the farther away from the sound source, the lower the rotation motion. At a diameter of 48 mm shows that the highest rotational motion is at a distance of 20 cm, which is equal to 257 rpm. Whereas for the lowest point is at a length of 35 cm from the sound source, which is 233 rpm. As with the 50 mm diameter, the tendency of the research results from the rotational motion is the farther away from the sound source, the turbine rotational motion will be lower. From the comparison chart, it is known that the impulse turbine with a diameter of 50 mm obtains higher results when compared to a diameter of 48 mm.

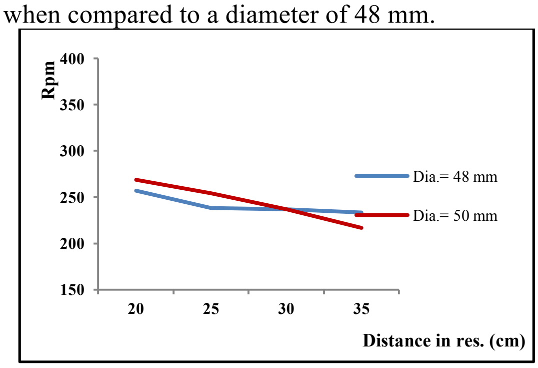

Fig. 6. Comparison Graph Of Impulse Turbine Rotational Motion With The Number Of Blades (Z) = 30.

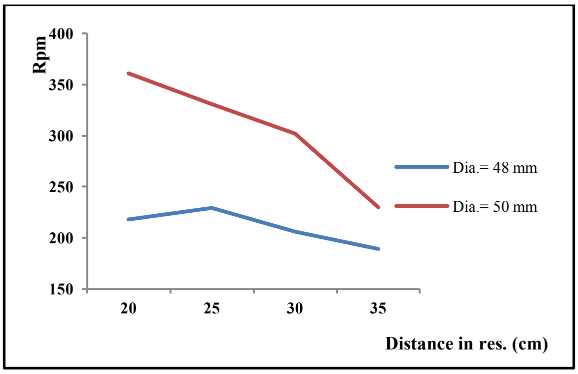

Fig. 7. Comparison Graph Of Impulse Turbine Rotational Motion With The Number Of Blades (Z) = 28.

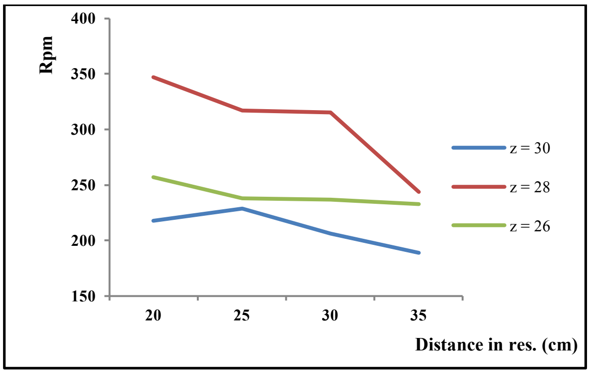

Fig. 9. The Rpm Of 48 Mm Diameter Turbine With Variations In The Number Of Blades (Z).

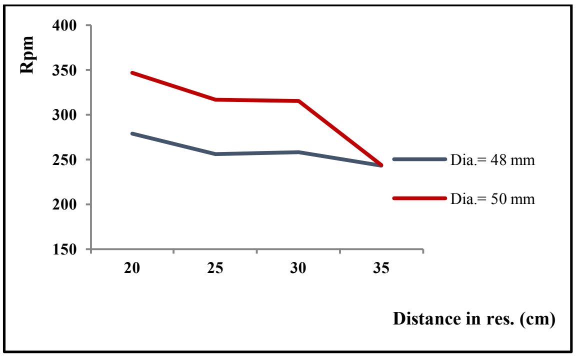

Fig. 8. Comparison Graph Of Impulse Turbine Rotational Motion With The Number Of Blades (Z) = 26.

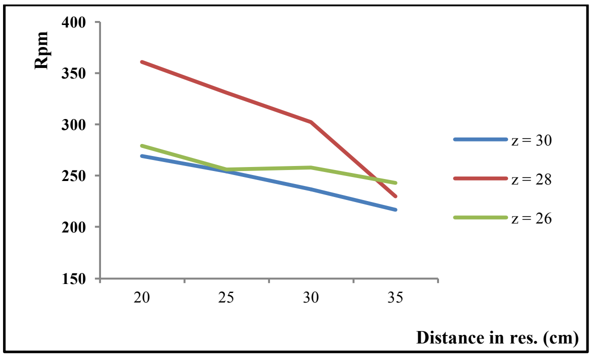

Fig. 10. The Rpm Of 50 Mm Diameter Turbine With Variations In The Number Of Blades (Z).

Based on the graph in Fig. 7, it is known that the comparison of impulse turbine motion with a diameter of 48 mm and 50 mm and the number of blades 28 shows that with a diameter of 50 mm it produces a higher rotational motion compared to a diameter of 48 mm. At a diameter of 50 mm, obtain the most optimal rotational motion at a distance of 20 cm, which is equal to 361 rpm. While for the lowest point is at a length of 35 cm from the source of sound that is equal to 230 rpm.

The graph shows that the rotational motion tends that the farther the distance from the source of the sound, the faster the rotation motion at a diameter of 50 mm. The impulse turbine with a diameter of 48 mm obtains the most optimal rotational motion at a distance of 25 cm from the sound source, which is equal to 229 rpm. Whereas for the lowest result is at 35 cm point with the rotational motion of 189 rpm. Thus it shows that with a diameter of 50 mm, the results are more optimal when compared to a diameter of 48 mm in the same number of blades, namely 28.

The graph in Fig. 8 shows that at a diameter of 50 mm, obtains the highest rotational motion; there is a distance of 20 cm from the sound source, which is equal to 279 rpm. The lowest point is at a length of 35 cm from the sound source with the rotational motion of 243 rpm. The impulse turbine with a diameter of 48 mm obtains the highest rotational motion of 347 rpm at a distance of 20 cm from the sound source. While for the lowest rate there is a distance of 35 cm from the sound source of 244 rpm. It can be concluded that the most optimal rotational motion on the impulse turbine with 26 blade numbers, the diameter of 48 mm.

From Fig. 6 to Fig. 8 it can be explained that the turbine rotational speed is higher at the test point close to the core of the thermoacoustic engine and further decreases to the test point near the end of the resonator due to the pressure characteristics of the open-end SWTE system work pressure magnitude also follows a high pattern at the closed end but small at the open end [30].

Based on Fig. 9 and Fig. 10, the results show that the diameter of turbine 50 is capable of producing turbine turns higher than the diameter of the turbine 48 mm because when sound waves arrive at the turbine, the more full the cross-section of the turbine, presented with a large diameter (in this study, a diameter of 50 mm), the more wave energy is absorbed in the turbine so that the sound energy is converted to higher mechanical energy. This condition is shown in the 50 mm turbine diameter, which has a higher rotational speed than the 48 mm turbine diameter.

Another factor that influences the turbine rotation is the number of turbine blades. The increasing number of turbines will cause the distance between turbine blades to be narrower; this results in the pressure and velocity of the wave energy generated by the thermoacoustic engine not being able to hit the turbine blade optimally. In the non-optimal condition, the turbine blades receive pressure, and the speed of the wave energy causes the turbine rotation that is produced is lower than the number of turbines that are less. However, the number of turbines that are too small will cause the turbine rotation is also low, and this is because the distance between the blade of the turbine that is widening will cause more wave energy to be passed out of the turbine system. This study shows the results that the number of blades is 28, where this number between 30 and 26 has the highest results. The results of the study indicate that the impulse turbine diameter of 50 mm with the number of blades 28 has the highest rotational motion. The resulting rotational motion is 361 rpm at a distance of 20 cm from the sound source. The speed of a particle is related to the cross-sectional area and impedance of the material. The speed of a particle is related to the cross-sectional area and impedance of the material. Acoustic impedance is the ratio of acoustic pressure to acoustic volume flow [31], so that with a larger cross-sectional area, the same amount of material impedance and the same amplitude pressure, the particle velocity will be higher too.

5. Conclusion

The results of this study can be concluded that the amount of turbine rotation that is inserted into the resonator has the same trend with the amount of pressure in the resonator. Open-closed SWTE produces pressure for ¼ wavelength so that the highest pressure is on the closed side and the lowest pressure is on the open side, the effect is that the character of the turbine rotational speed will also follow the character of the magnitude of the pressure. Turbine rotational speed concerning turbine diameter and the number of turbine blades are affected by acoustic impedance. A large turbine cross-sectional area will result in a higher turbine rotation, but a large number of turbine blades will give rise to a high inertance so that the turbine rotation is even lower. However, the decreasing number of turbine blades also affects the acoustic waves that can be absorbed by the turbine blades. So in this study, the diameter of a turbine with a high rotational speed of 50 mm compared to a diameter of 48 mm and the number of turbine blades 28 produced a higher turbine rotation compared to turbines with a total of 30 and 26 blades.

6. Aknowledgments

This work was partially supported by Penelitian Terapan Unggulan Perguruan Tinggi (PTUPT) Gadjah Mada University and internal research grand of Vocational School Gadjah Mada University 2018 scheme, for being financially supported on partial research.

7. References

[1] H. Babaei and K. Siddiqui, "Design and optimization of thermoacoustic devices," *Energy Convers. Manag.*, vol. 49, no. 12, pp. 3585–3598, 2008.

[2] K. De Blok, "Low operating temperature integral thermo acoustic devices for solar cooling and waste heat recovery," *J. Acoust. Soc. Am.*, vol. 123, no. 5, pp. 3541–3541, 2008.

[3] J. A. Mumith, C. Makatsoris, and T. G. Karayiannis, "Design of a thermoacoustic heat engine for low temperature waste heat recovery in food manufacturing: A thermoacoustic device for heat recovery," *Appl. Therm. Eng.*, vol. 65, no. 1–2, pp. 588–596, 2014.

[4] M. Hatazawa, H. Sugita, T. Ogawa, and Y. Seo, "Performance of a Thermoacoustic Sound Wave Generator driven with Waste Heat of Automobile Gasoline Engine.," *Trans. Japan Soc. Mech. Eng. Ser. B*, vol. 70, no. 689, pp. 292–299, 2011.

[5] D. Sahoo, A. Kotrba, T. Steiner, and G. Swift, "Waste Heat Recovery for Light-Duty Truck Application Using ThermoAcoustic Converter Technology," *SAE Int. J. Engines*, vol. 10, no. 2, pp. 196–202, 2017.

[6] S. Backhaus, E. Tward, and M. Petach, "Traveling-wave thermoacoustic electric generator," *Appl. Phys. Lett.*, vol. 85, no. 6, pp. 1085–1087, 2004.

[7] Z. H. Wu, M. Man, E. C. Luo, W. Dai, and Y. Zhou, "Experimental investigation of a 500 W traveling-wave thermoacoustic electricity generator," *Chinese Sci. Bull.*, vol. 56, no. 19, pp. 1975–1977, 2011.

[8] Z. Yu, A. J. Jaworski, and S. Backhaus, "Travelling-wave thermoacoustic electricity generator using an ultra-compliant alternator for utilization of low-grade thermal energy," *Appl. Energy*, vol. 99, pp. 135–145, 2012.

[9] M. Shalby, P. Walker, and D. G. Dorrel, "The Investigation of a Segment Multi-Chamber Oscillating Water Column in Physical Scale Model," in *5th International Conference on Renewable Energy Research and Applications, ICRERA 2016*, vol. 5, pp. 3–8, 2016.

[10] M. Mueller, R. Lopez, A. McDonald, and G. Jimmy, "Reliability analysis of wave energy converters," in *5th International Conference on Renewable Energy Research and Applications, ICRERA 2016*, vol. 5, pp. 667–672, 2016.

[11] M. Sanada, Y. Inoue, and S. Morimoto, "Generator design and characteristics in direct-link wave power generating system considering appearance probability of waves," in *1st International Conference on Renewable Energy Research and Applications (ICRERA)*, pp. 1–6, 2012.

[12] M. Takao, M. M. A. Alam, Y. Kinoue, K. Yamada, S. Okuhara, and S. Nagata, "Counter-rotating Impulse Turbine for Wave Energy Conversion," in *6th International Conference on Renewable Energy Research and Application, ICRERA 2017*, vol. 5, pp. 3–6, 2017.

[13] T. Setoguchi and M. Takao, "Current status of self rectifying air turbines for wave energy conversion," *Energy Convers. Manag.*, vol. 47, no. 15–16, pp. 2382–2396, 2006.

[14] H. Canilho and C. Fael, "Velocity Field Analysis of a Channel Narrowed by Spur-dikes to Maximize Power Output of In-stream Turbines," *J. Sustain. Dev. Energy, Water Environ. Syst.*, vol. 6, no. 3, pp. 534–546, 2018.

[15] B. Pereiras, F. Castro, A. el Marjani, and M. A. Rodríguez, "An improved radial impulse turbine for OWC," *Renew. Energy*, vol. 36, no. 5, pp. 1477–1484, 2011.

[16] S. K. Mishra, S. Purwar, and N. Kishor, "An optimal and non-linear speed control of oscillating water column wave energy plant with wells turbine and DFIG," *Int. J. Renew. Energy Res.*, vol. 6, no. 3, pp. 995–1006, 2016.

[17] M. M. A. Alam, A. Takami, M. Takao, Y. Kinoue, S.

Okuhara, and T. Setoguchi, "Wells turbine with booster: Effect of rotational speed ratio on the performance," in *5th International Conference on Renewable Energy Research and Applications, ICRERA 2016*, vol. 5, pp. 11–15, 2016.

[18] T. Karthikeyan, A. Samad, and R. Badhurshah, "Review of air turbines for wave energy conversion," in *International Conference on Renewable Energy and Sustainable Energy, ICRESE 2013*, pp. 183–191, 2013.

[19] T. Kloprogge, "Turbine Design for Thermoacoustic Generator," 2012.

[20] E. T. Boessneck and T. E. Salem, "Performance Characterization of Bi-Directional Turbines for Use in Thermoacoustic Generator Applications," p. V001T09A001, 2016.

[21] C. Shen, Y. He, Y. Li, H. Ke, D. Zhang, and Y. Liu, "Performance of solar powered thermoacoustic engine at different tilted angles," *Appl. Therm. Eng.*, vol. 29, no. 13, pp. 2745–2756, 2009.

[22] G. .Swift, "Thermoacoustics : A Unifying Perspective for Some Engines and Refrigerators," *Leb. und-Technologie*, vol. 35, no. 7, p. 636, 2002.

[23] P. Puddu, M. Paderi, and C. Manca, "Aerodynamic characterization of a wells turbine under bi-directional airflow," *Energy Procedia*, vol. 45, pp. 278–287, 2014.

[24] A. Thakker and F. Hourigan, "Modeling and scaling of the impulse turbine for wave power applications," *Renew. Energy*, vol. 29, no. 3, pp. 305–317, 2004.

[25] Sugiyanto, S. Kamal, J. Waluyo, and A. Widyaparaga, "Simulation of Close-Open Standing Wave Thermoacoustic Engine Toward Variation of Resonator Diameter," in *4th International Conference on Science and Technology, ICST 2018*, Yogyakarta , vol. 1, pp. 1–5, 2018

[26] M. Skaria, K. K. Abdul Rasheed, K. A. Shafi, S. Kasthurirengan, and U. Behera, "Simulation studies on the performance of thermoacoustic prime movers and refrigerator," *Comput. Fluids*, vol. 111, pp. 127–136, 2015.

[27] T. Biwa, Y. Tashiro, H. Nomura, Y. Ueda, and T. Yazaki, "Experimental verification of a two-sensor acoustic intensity measurement in lossy ducts," *J. Acoust. Soc. Am.*, vol. 124, no. 3, pp. 1584–1590, 2008.

[28] F. Jacobsen, "On the uncertainty in measurement of sound power using sound intensity," *Noise Control Eng. J.*, vol. 55, no. 1, p. 20, 2008.

[29] T. Harčarik, J. Bocko, and K. Masláková, "Frequency analysis of acoustic signal using the Fast Fourier Transformation in MATLAB," *Procedia Eng.*, vol. 48, pp. 199–204, 2012.

[30] K. Tourkov and L. Schaefer, "Effect of regenerator positioning on thermoacoustic effect in a looped tube traveling wave thermoacoustic engine," *Energy Convers. Manag.*, vol. 95, pp. 94–100, 2015.

[31] T. D. Rossing, *Springer Handbook of Acoustic*. LLC New York: Springer Science+Business Media, 2007.